Rostral Versus Caudal Differences in Mechanical Entrainment of the Lamprey Central Pattern Generator for Locomotion

Eric D. Tytell and Avis H. Cohen

J Neurophysiol 99:2408-2419, 2008. First published 6 February 2008; doi:10.1152/jn.01085.2007

Journal of Neurophysiology publishes original articles on the function of the nervous system. It is published 12 times a year (monthly) by the American Physiological Society, 9650 Rockville Pike, Bethesda MD 20814-3991. ISSN: 0022-3077, ESSN: 1522-1598. Visit our website at http://www.the-aps.org/.

J Neurophysiol 99: 2408–2419, 2008.
First published February 6, 2008; doi:10.1152/jn.01085.2007.

Rostral Versus Caudal Differences in Mechanical Entrainment of the Lamprey Central Pattern Generator for Locomotion

Eric D. Tytell[1] and Avis H. Cohen[1,2]
[1]*Department of Biology and* [2]*Institute for Systems Research, University of Maryland, College Park, Maryland*

Submitted 28 September 2007; accepted in final form 2 February 2008

Tytell ED, Cohen AH. Rostral versus caudal differences in mechanical entrainment of the lamprey central pattern generator for locomotion. *J Neurophysiol* 99: 2408–2419, 2008. First published February 6, 2008; doi:10.1152/jn.01085.2007. In fishes, undulatory swimming is produced by sets of spinal interneurons constituting a central pattern generator (CPG). The CPG generates waves of muscle activity that travel from head to tail, which then bend the body into wave shapes that also travel from head to tail. In many fishes, the wavelengths of the neural and mechanical waves are different, resulting in a rostral-to-caudal gradient in phase lag between muscle activity and bending. The neural basis of this phase gradient was investigated in the lamprey spinal cord using an isolated in vitro preparation. Fictive swimming was induced using D-glutamate and the output of the CPG was measured using suction electrodes placed on the ventral roots. The spinal cord was bent sinusoidally at various points along its length. First, the ranges of entrainment were estimated. Middle segments were able to entrain to frequencies approximately twice as high as those at end segments. Next, phase lags between centers of ventral root bursts and the stimulus were determined. Two halves of the cycle were identified: stretching and shortening of the edge of spinal cord on the same side as the electrode. Stimuli at rostral segments tended to entrain segmental bursting at the beginning of the stretch phase, almost 50% out of phase with previously measured in vivo electromyography data. Stimuli at caudal segments, in contrast, entrained segments at the end of stretch and the beginning of shortening, approximately the same phase as in vivo data.

INTRODUCTION

In vertebrates, the basic pattern for rhythmic movements like swimming and walking is generated by a group of spinal interneurons that form a locomotor central pattern generator (CPG; Cohen and Wallén 1980). The vertebrate locomotor CPG consists of repeated oscillatory subunits, each of which generates bursts that are phase-locked to the other oscillators (Grillner 1985). In the lamprey, for instance, unit oscillators repeat segmentally and maintain a consistent phase offset, producing a traveling wave of neural activity that activates the axial muscles, producing the undulatory swimming wave (Wallén and Williams 1984).

Although the CPG can generate this rhythm independently of sensory input, it is strongly affected by sensory information, particularly proprioceptive inputs. Impulsive stimuli can reset the CPG rhythm (McClellan and Jang 1993). Rhythmic stimuli tend to cause CPG burst frequency to approach the stimulus frequency, a phenomenon called entrainment (Grillner 1974; Marder and Bucher 2001). Proprioception in the lamprey is mediated by stretch receptive neurons called edge cells that are located on the margins of the spinal cord (Grillner et al. 1984). Edge cells are similar to mammalian spindle organs in their properties and their effect on the CPG (Viana Di Prisco et al. 1990): they respond to both static stretch and the rate of stretch (Grillner et al. 1982), inhibiting the contralateral CPG unit while exciting the ipsilateral one (Viana Di Prisco et al. 1990). Like spindle organs, they receive phasic inhibition from the CPG, which reduces their excitability in phase with the CPG output. This inhibition potentially removes some of the influence of the excitation that would be caused by self-imposed body bending (Vinay et al. 1996), much like the inhibition of spindle organs during stepping (Gossard 1996). The proprioceptive organ is not known in other fishes, except for elasmobranchs (Bone 1978).

Sensory feedback and entrainment of the locomotor CPG are functionally important in fishes and tetrapods to correct for perturbations (McClellan and Jang 1993; Pearson 1995) and to tune the locomotory rhythm to the mechanical properties of the body and environment (Guan et al. 2001; Hatsopoulos and Warren 1996; Iwasaki and Zheng 2006; Williams and DeWeerth 2007). More generally, proprioceptive sensory input influences the relative timing of body movement and CPG activity and thus the timing of muscle activity relative to body movement. This phase relationship can have profound consequences for energy use and force output. When muscles are activated as they are shortening, they produce energy for locomotion but have relatively low forces (McMahon 1984). In contrast, when muscles are active while they are forcibly stretched, they absorb energy but produce much higher forces (McMahon 1984).

It may be that different segments along the spinal cord respond differently to sensory inputs. Nonetheless, unit oscillators in the CPG have often been assumed to be identical, both in their intrinsic properties and in their response to sensory input. This simplifying assumption has been essential in producing mathematical models of the CPG (e.g., Cohen et al. 1982; Ekeberg and Grillner 1999; Williams 1992), but there is some evidence that it may not be valid. The intrinsic frequencies of CPG oscillators appear to differ along the spinal cord, possibly varying randomly (Cohen 1987) or with a gradient (Hagevik and McClellan 1999). Additionally, rostral segments entrain over a narrower range of frequencies than caudal segments (McClellan and Sigvardt 1988; Williams et al. 1989).

Other evidence for the variation in the CPG's response to stimuli comes mostly from electromyographic studies of freely

Address for reprint requests and other correspondence: E. D. Tytell, Department of Biology, Biology/Psychology Building, University of Maryland, College Park, MD 20742 (E-mail: tytell@umd.edu).

The costs of publication of this article were defrayed in part by the payment of page charges. The article must therefore be hereby marked "*advertisement*" in accordance with 18 U.S.C. Section 1734 solely to indicate this fact.

swimming fishes (Wardle et al. 1995). For example, in the lamprey, the CPG generates a wave of neural activity with a wavelength slightly longer than the body length (Williams et al. 1989). This neural wave activates the axial musculature, generating force to bend the body, but the resulting curvature has a wavelength of only about 0.7 body lengths (Williams et al. 1989). Because of the different wavelengths of the neural and mechanical waves, the phase relationship between them changes along the length of the body. Close to the head, the CPG activates the muscle on one side of the body just after it has been maximally stretched, so that it shortens while it is active (called a "concentric" contraction; McMahon 1984) and produces energy for locomotion. Close to the tail, however, muscle segments turn on later relative to bending, first shortening slightly then being forcibly stretched (called an "eccentric" contraction), which generates little net work or even absorbs energy (Wardle et al. 1995).

Although the presence and physical consequences of the phase shift have been debated extensively, a different but related question has received little attention. Is the phase difference a result of rostral-to-caudal differences in the CPG itself or is it a consequence of body and fluid properties? Some of the lag could be a consequence of the variation in body shape along a fish's length. In the lamprey, the greater thickness of the rostral body causes it to be stiffer than the caudal area, whereas the dorsal and anal fins in the caudal regions cause them to have a higher fluid dynamic drag coefficient. These physical differences could alter the phase relationship between muscle force and body bending. Additionally, the length and velocity dependence of muscle (McMahon 1984) could have an effect. Because of the higher amplitude near the tail, the caudal muscles must produce faster and larger contractions than rostral muscles (Rome et al. 1993). On the other hand, proprioceptors or the segmental oscillators themselves may respond to bending at different phases, encoding the phase shift neurally.

Therefore in this study we investigate how the lamprey CPG entrains to mechanical stimuli at different locations along the spinal cord. We examine both entrainment ranges and the phase relationship between CPG activity and an imposed sinusoidal bending stimulus. This question was preliminarily addressed by Sigvardt and Williams (1989) who found that a bending stimulus applied to the rostral end of a isolated spinal cord preparation will entrain the CPG at a different phase offset than when the same stimulus is applied to the caudal end (reviewed in Williams et al. 1995). The phase differences they observed were similar to those seen in freely swimming animals.

We follow up their work in more detail, examining the phase relationship between bending and CPG bursting at many points along the isolated lamprey spinal cord. We address two alternative hypotheses about how the phase gradient could arise. First, such differences could be an artifact of the dissection procedure. Because a portion of the spinal cord is cut out during the dissection, the rostral end of the preparation receives more ascending inputs than descending and the caudal end receives more descending inputs than ascending. Under this hypothesis, even though CPG oscillators and edge cells are equivalent along the length of the spinal cord, the differences in ascending and descending coupling (Kiemel et al. 2003; McClellan and Hagevik 1999; Williams et al. 1990) cause the CPG to respond differently to stimulation at the rostral or caudal ends of the preparation. In this case, any excised section of spinal cord should display a gradient, even if all of the segments are from the tail region of the animal.

Alternatively, some aspect of the edge cells or the CPG itself may differ at different anatomical locations (as has been observed in *Xenopus* embryos; Tunstall and Roberts 1994). If the spinal cord does have some sort of anatomical heterogeneity like this, then sections of the cord from different locations should entrain to bending at different phases, regardless of the length of the section. By examining entrainment in progressively shorter sections of the spinal cord, we are able to distinguish between our two mechanistic hypotheses.

Preliminary results of this study have been published in abstract form (Tytell and Cohen 2007).

METHODS

Fictive swimming protocol

Adult lampreys, *Ichthyomyzon unicuspis*, were obtained from fishermen along Lake Michigan (U.S.) and kept in aerated aquaria at 4°C.

The dissection protocol was as follows. Animals were first anesthetized using buffered MS222 (0.2 g/l) then rapidly decapitated and eviscerated. The skin and muscle were peeled away from the notochord. Approximately 50 spinal segments, from the last gill slit to the anus, were exposed. Care was taken to avoid damaging the motor nerves, which run along the notochord, when removing the muscle tissue. All membranes dorsal to the spinal cord were removed and the preparation was transferred to a bath of physiological saline (NaCl, 91 mM; KCl, 2.1 mM; $CaCl_2 \cdot 2H_2O$, 222.6 mM; $MgCl_2 \cdot 6H_2O$, 1.8 mM; glucose, 4.0 mM; $NaHCO_3$, 20.0 mM) at 9°C. Oxygen was occasionally bubbled through the saline.

Fictive swimming was induced using D-glutamate at concentrations ranging from 0.35 to 1 mM, adjusting the concentration to achieve a stable rhythm. Resulting frequencies ranged from 0.5 to 1.3 Hz and had no apparent correlation with glutamate concentration. Once an experiment was started, the glutamate concentration was kept constant. CPG output was measured either at the ventral roots inside the spinal cord canal or the motor nerves on the outside of the notochord, using glass suction microelectrodes filled with saline. At least two electrodes were used for each preparation. Signals from the electrodes were amplified and filtered using a differential amplifier (Model 1700, A–M Systems, Carlsborg, WA). The signals were then digitized at 5 kHz using a data acquisition card (PCI-6221, National Instruments, Austin, TX) and stored to disk for later analysis.

All animal procedures were approved by the University of Maryland Institutional Animal Care and Use Committee (approval number R-R-05-46).

Terminology

To avoid confusion, the terms "rostral" and "caudal" are used throughout only to mean the rostral and caudal ends of the preparation, even if all segments in the preparation come from the tail region (i.e., the anatomically caudal end of the body). We will refer to anatomically rostral and caudal segments as coming from the "head" or "tail" region. Finally, when the stimulus is rostral to the recording site, it will be called "above" or "higher" than the recording, whereas a stimulus caudal to the recording site will be called "below" or "lower" than the recording.

Bending

The preparation was set up for bending stimulation by pinning part of it securely through the notochord, leaving a portion of the spinal

cord and notochord free to bend (Fig. 1). At the pivot point, two pairs of pins were used to ensure that the preparation remained motionless (Fig. 1*A*). One electrode was placed one or two segments away from the pivot point. The free end of the notochord was then secured to a motorized arm using loosely attached stainless steel clips (1 cm wide; Fig. 1*A*). When the free end was long (>20 segments), multiple clips were used to keep the entire section straight, except for the one or two segments adjacent to the pivot point (Fig. 1*B2*). The arm was connected via a timing belt to a computer-controlled motor [CX-660 pen motor controller (GSI-Lumonics, Bedford, MA) or MD2S microstepping motor controller (US Digital, Vancouver, WA)]. The angle of the motor arm was controlled by computer, using the data acquisition card and the Matlab R2006b Data Acquisition Toolbox (The MathWorks, Natick, MA). To avoid damaging the preparation, the number of times the notochord was pinned or unpinned was kept to a minimum. Within this constraint, however, stimulus positions were tested in as random an order as possible. After four or five stimulus positions were tested, the preparation was shortened by removing approximately 10 segments, repeating the stimulus, and, in several preparations, removing ten more segments and repeating the stimulus yet again (Fig. 1*B3*). For stimuli below the recording site, caudal segments were clipped, whereas for stimuli above the electrode, rostral segments were clipped. The initial, approximately 50-segment-long preparation is referred to as the "whole" preparation, whereas the subsequent preparations are referred to as "shortened" preparations.

For each preparation and stimulus position, the rhythmic output of the spinal cord was monitored for 10 min under control conditions to estimate the initial resting frequency $f_{rest,0}$. The resting frequency f_{rest} was also estimated during all other times without bending stimulation. For simplicity, stimulus frequency was normalized by the average resting frequency across all unstimulated periods in an entire recording bout (typically 10 to 15 min long).

Bending stimuli were applied using two procedures. First, to estimate the approximate range over which the bending stimulus could entrain the CPG rhythm, a "frequency sweep" protocol was used. Stimulus frequency was gradually increased or decreased in a stepwise fashion, maintaining an individual frequency for 10 cycles. The range of frequencies was generally from 0.5 to 1.5 times the initial resting frequency, although a narrower frequency range was sometimes used if the CPG was clearly not able to entrain at the higher or lower frequencies. Entrainment ranges were determined manually by examining both whether the burst frequency matched the stimulus frequency and whether a constant phase relationship was maintained (Fig. 3). Second, the stimulus was turned on and off several times (at least five) at a given frequency known to cause entrainment, keeping the stimulus on for 30 cycles and then off for ≥30 s. This protocol allowed multiple statistically independent estimates of burst phase. Because of the intrinsic variability in burst times, these "isolated trials" each started at a random phase in the CPG burst period. This randomness ensured that the measured phase relative to the stimulus was not a function of the initial conditions, but was instead specific to the CPG at that stimulus position and frequency.

In all cases the total angular displacement of the arm (from maximum displacement on one side to maximum displacement on the other) was 36°. This amplitude was chosen by reviewing previous studies (Kiemel and Cohen 2001; Williams et al. 1990) for an amplitude that would consistently cause entrainment. Usually at least three different frequencies were tested in isolated trials: two frequencies at the lower and upper end of the entrainment range, respectively, and one or more near the resting frequency. The same frequency was presented at least five times in a row, with the order of frequencies randomized.

Frequency analysis

Post hoc signal analysis was performed using Matlab. Spikes were first detected using a manually set threshold, then bursts were located by analyzing mean spike time within a sliding time window, chosen to be 80% of the estimated burst period. A burst was detected when the mean spike time within the window crossed the center of the window with a negative slope. Figure 2*A* shows a schematic of the burst-finding procedure. The burst time was defined as the mean spike time within the burst (i.e., the center of the burst).

Entrainment was defined as periods when the burst frequency on all electrodes approached within 5% of the stimulus frequency and, at the same time, when the phase of each burst deviated by <5% from the mean phase over the five bursts before and five bursts after it. In principle, during entrainment, the burst frequency should be exactly equal to the stimulus frequency. However, estimates of burst times always contain some error and CPG burst times themselves have noise (Cohen and Wallén 1980; Kiemel and Cohen 1998). Thus 5% frequency deviation was chosen as a reasonable cutoff for entrainment. Note that this definition of entrainment is equivalent to 1:1 entrainment, as used in previous studies (e.g., McClellan and Sigvardt 1988; Williams et al. 1990) because one burst occurs per stimulus cycle. The detailed analyses subsequently described were performed only on data from the electrode closest to the bending site.

To determine whether entrainment ranges differed among stimulus positions, a mixed-model regression analysis was performed (also

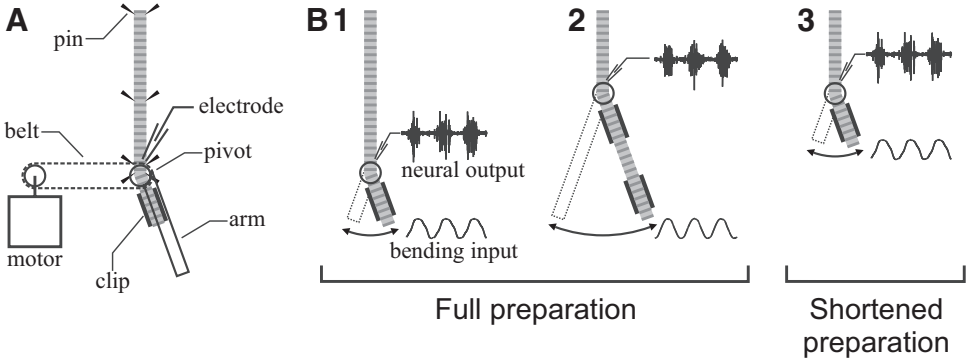

FIG. 1. Methods. *A*: general setup. Fifty segments of notochord and spinal cord are pinned down in a Sylgard dish containing chilled physiological saline. A pivot point is pinned with 2 pairs of pins to ensure that it does not move. The free end is connected using a stainless steel clip to an arm, which is in turn connected by a belt to a motor. A computer controls the motor and records output from an electrode placed close to the pivot point. *B1* and *B2*: the bending stimulus was applied at various positions along the length of the cord, taking care to hold the moving section straight. *B3*: more central stimulus locations were also tested by clipping the long free section. These procedures were performed in 2 ways: as illustrated, with the stimulus below (caudal to) the recording site, and also in reverse, with the stimulus above (rostral to) the recording site. When the stimulus was below (above) the electrode, the preparation was shortened by clipping off caudal (rostral) segments.

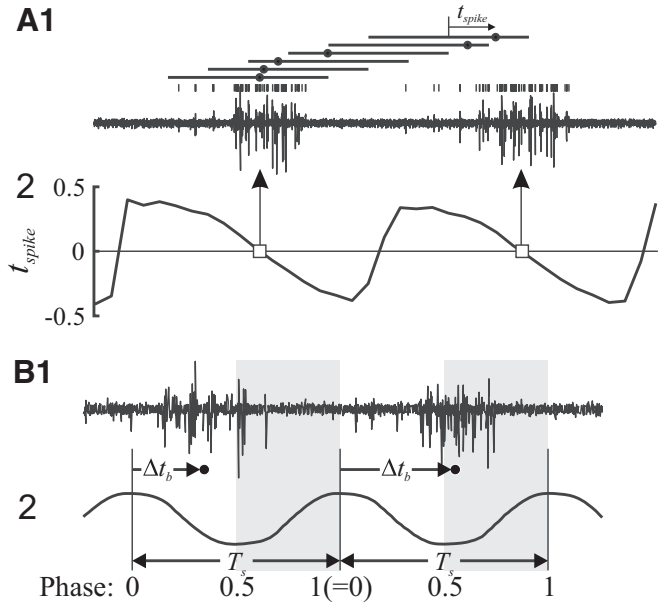

FIG. 2. Data analysis. *A*: schematic of the burst finding method. First, spikes (shown as vertical bars in *panel 1*) are located according to a manual threshold. Then, the mean spike time within a sliding window is estimated. Example windows with mean spike times are shown as horizontal bars and circles, respectively, above the spikes. Mean spike time t_{spike} is defined relative to the center of each window. Bursts are located when t_{spike} crosses zero with a negative slope (squares in *panel 2*). *B*: definition of phase. *Trace 1* shows an example ventral root recording; *trace 2* shows the stimulus. For each burst in the *top trace*, the burst time is estimated as the mean of the spike times within the burst (circles). Stimulus cycles are defined as the period T_s from one maximum excursion on the same side as the recording to the next (vertical lines). For each burst, Δt_b is defined as the duration between the burst time and the time when the stimulus was last at its maximum excursion on the same side as the electrode. The phase (bottom axis) is thus equal to $\Delta t_b/T_s$ and ranges from 0 to 1, where 0 to 0.5 indicates that the burst is centered during the time when ipsilateral muscle would be lengthening, whereas 0.5 to 1 (gray region) indicates that ipsilateral muscle would be shortening.

called ANCOVA; Milliken and Johnson 2001). Fixed effects in the model were the stimulus position and position squared. The individual was included as a random categorical effect. Interaction terms with the individual effect were included only if the main effects were significant (Milliken and Johnson 2001). Statistics were performed using Matlab's *anovan* function.

Isolated trials were used to determine an approximate entrainment probability. Each 30-cycle trial was classified as entrained or not, based on the preceding criteria. Stimulus frequencies were collected into 10 bins across each entrainment range, estimated using a frequency sweep. The number of isolated trials in each frequency bin divided by the total number of trials in that bin defined an approximate probability of entrainment.

Phase analysis

The phase at the center of the burst was defined relative to the stimulus, subtracting the time at which the stimulus last reached its maximum position on the same side as the electrode and dividing by the stimulus period. Phase values thus ranged from 0 to 1; values from 0 to 0.5 indicate that the center of the burst occurs when the muscle on that side of the body (ipsilateral) would be lengthening, whereas values from 0.5 to 1 indicate when the ipsilateral muscle would be shortening. Figure 2*B* illustrates the definition of phase. It should be noted that bursts typically last about 30% of a cycle (Wallén and Williams 1984); thus a phase value of 0.5 at the center of the burst means that the burst occurs for about 15% of the cycle during lengthening and about 15% during shortening. Statistics on phase measurements were performed using circular algorithms, implemented in Matlab, based on those described by Fisher (1995).

At least five isolated trials of bending at the resting burst frequency were conducted at each position. The median phase (Fisher 1995) in each trial was estimated, using the median to avoid influence of the early period of each trial in which the phase converged to its steady value (e.g., Fig. 3*B*). Then, for each individual and stimulus position, all trials were averaged and compared among stimulus positions and preparation types (whole vs. shortened). Comparisons were performed using a nonparametric circular test for a common median among groups (Fisher 1995). For all N data points, estimate the median phase Θ. Then m_i is the number of phase values in group i between $\Theta - 0.5$ and Θ. Also let $M = m_1 + m_2 + \ldots + m_r$, where r is the number of groups. The test statistic is

$$P_r = \frac{N^2}{M(N-M)} \sum_{i=1}^{r} \left[\frac{m_i^2}{n_i} - \frac{NM}{(N-M)} \right] \quad (1)$$

where n_i is the number of values in group i. According to Fisher (1995), P_r is distributed as χ^2_{r-1}. If the groups were significantly different, pairwise comparisons were performed using the same test with a Bonferroni correction to avoid false positives arising from multiple comparisons (Zar 1999).

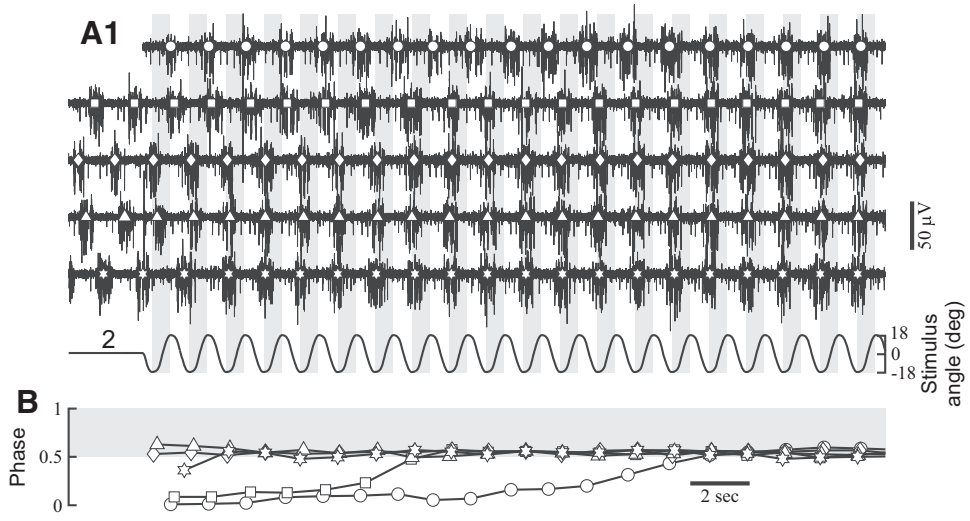

FIG. 3. An example of entrainment. Final entrainment phase is consistent regardless of the initial phase relationship between bursts and the stimulus. Both panels show the same 5 successive presentations of a bending stimulus at 0.79 Hz to a cord with a resting frequency of 0.73 Hz. *A*: ventral root recordings (*panel 1*) and stimulus angle (*panel 2*). Bursts are marked with open symbols and the shortening phase of bending is indicated with gray bars. *B*: phase of the bursts with respect to bending. Symbols are the same as in *A*. Phase from 0 to 0.5 indicates lengthening on the side of the electrode, whereas 0.5 to 1 indicates shortening.

RESULTS

In all, 10 individuals (total length: 25 to 33 cm; mean 28 ± 1 cm) were used throughout this study. For each individual, bending stimuli were tested at four or more positions along the preparation.

The CPG burst frequency was first measured using an electrode at a position close to the stimulus (within two segments) without bending stimuli to determine the initial resting frequency. This frequency was not constant during the experiment; it tended to increase after bending stimuli. After each round of entrainment, the burst frequency would decay back toward the resting frequency, but would stabilize slightly above it, similar to the effect described by Kiemel and Cohen (2001) and McClellan and Sigvardt (1988). The frequency increase was sometimes quite long-lasting, gradually returning to the initial resting frequency over the course of many minutes (data not shown). Sham tests were performed in which the bath was stirred at the bending frequency without actually bending the spinal cord; no frequency increase was observed (data not shown). For simplicity, stimulus frequency throughout is normalized by the mean resting frequency over the course of a bout of stimulation.

Figure 3 shows an example of entrainment during an isolated trial. Thirty cycles of a stimulus at $1.08f_{rest}$ were applied, then the stimulus was turned off for 30 s. This procedure was repeated five times (shown as successive rows is Fig. 3*A1*). In each case, burst phase stabilized at about 0.5, although it took 14 bursts in the first case. Note that the one trace that took such a long time to converge in Fig. 3*B* is an extreme example: burst phase generally converged much more rapidly, usually within one or two cycles, like the other traces in Fig. 3.

Entrainment ranges

Entrainment as shown in Fig. 3 could be produced over a range of stimulus frequencies. The entrainment range was determined by gradually increasing or decreasing the stimulus frequency. At each position, such "frequency sweeps" generally produced clear entrainment in the entire spinal cord over a range of bending frequencies (Fig. 4*A1*). Stimulation at frequencies beyond the entrainment range often produced highly variable burst frequencies (note the burst frequencies at times just before and after entrainment in Fig. 4*A1*). As stimulus frequency changed, the phase relationship between bursts and the bending stimulus changed (Figs. 4*A2* and 4*B*). In the current convention for phase, phase generally increased with increasing frequency or decreased with decreasing frequency.

Figure 5 shows all measured entrainment ranges plotted against the stimulus position. In total, 83 frequency sweeps were performed, 63 with frequency increasing and 20 with frequency decreasing. Occasionally, the first or last frequency tested in a sweep caused entrainment, which meant that only one bound could be determined unambiguously (15 lower bounds and 12 upper bounds; circles in Fig. 5). Frequency sweeps with increasing or decreasing frequency did not produce different upper or lower bounds (paired *t*-test; $P = 0.30$, $n = 16$; data not shown) and are therefore considered together. In general, upper bounds tended to be highest for stimulus positions near the middle of the spinal cord, whereas lower bounds did not show systematic variation with position. To test this observation, each bound was regressed against stimulus position and stimulus position squared. The individual was included as a random, categorical effect (Milliken and Johnson 2001) to estimate and control for individual variance in the population. Table 1 shows the results of this analysis. Upper bounds had a significant relationship to position and position squared, whereas lower bounds had no significant relationship to position (Fig. 5). The estimated population SD was substantially larger for the upper bounds: $0.10f_{rest}$ for the upper bound and $0.048f_{rest}$ for the lower.

These entrainment ranges do not appear to define strict boundaries within which entrainment always occurred, but rather regions of high probability of entrainment. Because two different stimulation protocols were used (frequency sweeps and isolated trials), the isolated trials could be used to probe the properties of entrainment ranges as determined by frequency sweeps. Figure 6 shows the estimated probability of entrainment for isolated trials at specific frequencies. In Fig. 6*A*, frequency has been normalized by the entrainment range (determined by a frequency sweep) for the specific individual and stimulus position, so that 0 and 1 respectively represent the lower and upper bounds of entrainment. In isolated trials, entrainment was possible at normalized frequencies below 0 or above 1, but it was less likely than entrainment at frequencies between 0 and 1. Additionally, entrainment is more likely at the upper end of the frequency range than at the lower end. In Fig. 6*B*, frequency has been normalized by the resting frequency, showing that entrainment is much less likely below

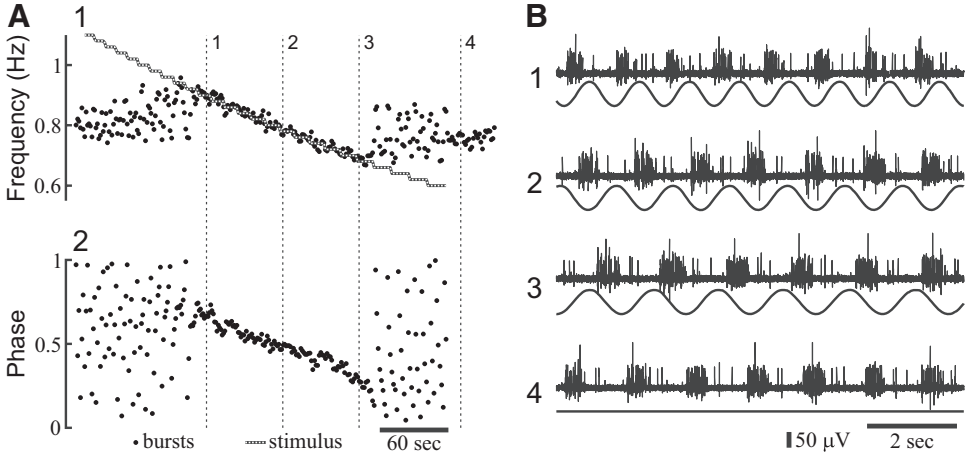

FIG. 4. The spinal cord entrains to a range of bending frequencies, but burst phase relative to the stimulus changes as bending frequency changes. *A*: burst and stimulus frequency (*panel 1*) and burst phase relative to the stimulus (*panel 2*). Vertical dashed lines indicate the times of corresponding numbered traces in *B*. Stimulus frequency ranged from 1.75 to $0.75f_{rest}$, where f_{rest} was 0.8 Hz. *B*: example traces from *A*. *Top traces* are ventral root recordings. *Bottom traces* are the stimulus angle. Note the changing phase relationship.

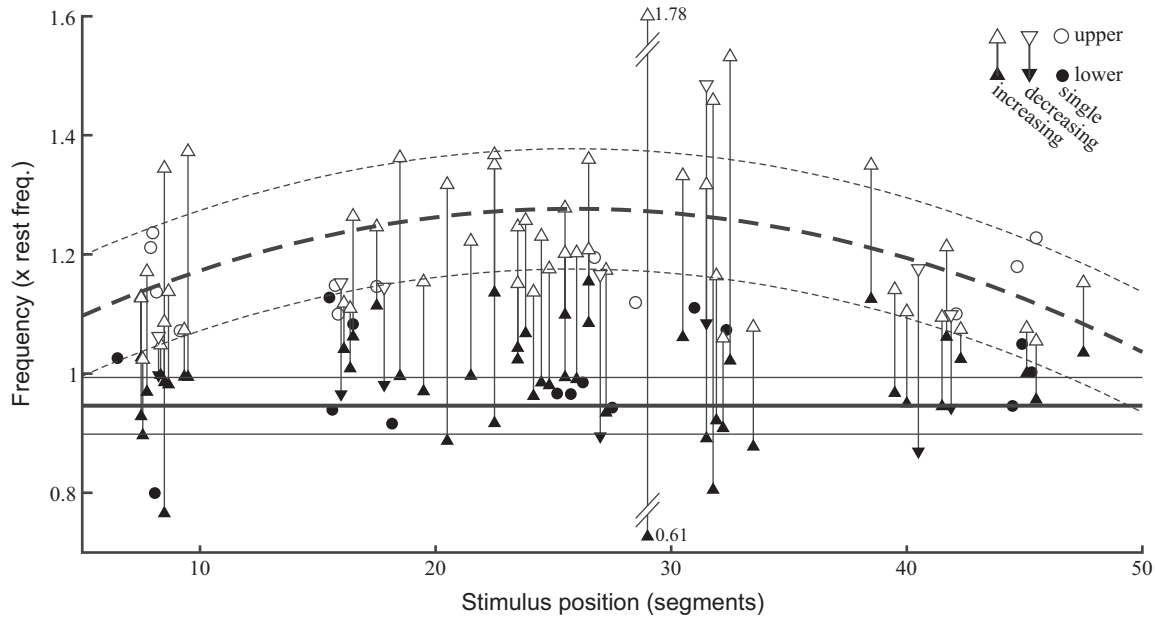

FIG. 5. Maximum entrainment frequency is higher at middle segments relative to the rostral or caudal end. Entrainment ranges were determined by gradually increasing or decreasing bending frequency and noting when burst frequency matched the bending frequency. Lower and upper bounds are shown with closed and open symbols, respectively, and vertical lines connect the bounds from the same test. Tests with increasing or decreasing frequency are indicated with up or down triangles, respectively. Sometimes only a lower or upper bound could be determined in a test; these are shown with closed and open circles, respectively. Thick solid and dashed lines show the significant terms from the regression of lower and upper bounds against position. Thin lines around the regression lines indicate the estimated population SD. One outlier is shown truncated. Data are from whole and shortened preparations.

than above the resting frequency (as previously observed; McClellan and Sigvardt 1988; Williams et al. 1990).

Rostral-to-caudal phase differences

At a given frequency and stimulus position, the burst phase during entrainment returned to the same approximate value. For an example, see Fig. 3*B*. To determine whether different portions of the spinal cord responded at different phases to a bending stimulus, the burst phase was estimated during bending close to the resting frequency. For each individual and position, at least five separate trials containing 30 cycles of bending were performed. The angular median burst phase in each trial was estimated. Each trial was assumed to be statistically independent of the others. Figure 7*A* shows example ventral root recordings during rostral and caudal entrainment from two different individuals (Fig. 7, *A1* and *A2* from one individual; Fig. 7, *A3* and *A4* from another). Figure 7*B1* shows mean phase for whole preparations ($n = 47$), whereas Fig. 7*B2* shows the means for shortened preparations ($n = 15$). Throughout the figure, closed symbols indicate whole preparations, whereas open symbols represent shortened preparations. Squares indicate that the stimulus was below (caudal to) the recording site, whereas circles indicate a stimulus above (rostral to) the recording.

Stimuli near the head resulted in different burst phases than those near the tail. For each individual animal, there was a discrete transition between the two phase values at some segment near the middle of the preparation. Because this transition point differed among preparations, the phase values at middle segments show a mixture of both phases (Fig. 7*B*). In

TABLE 1. *Results of regression analysis*

Source	Type	*SS*	df_1	*MS*	*F*	df_2	*P*
			A. Lower bound				
position	Fixed	0.0017	1	0.0017	0.27	59	0.608
position^2	Fixed	0.0006	1	0.0006	0.10	59	0.750
individual	**Random**	**0.1981**	**9**	**0.0220**	**3.50**	**59**	**0.002**
error		0.3714	59	0.0062			
			B. Upper bound				
position	**Fixed**	**0.1609**	**1**	**0.1609**	**11.77**	**10.98**	**0.006**
position^2	**Fixed**	**0.1554**	**1**	**0.1554**	**13.72**	**12.38**	**0.003**
individual	Random	0.1085	9	0.0121	1.38	38	0.231
position × individual	Random	0.1309	9	0.0145	1.67	38	0.131
position^2 × individual	Random	0.1076	9	0.0120	1.37	38	0.235
error		0.3314	38	0.0087			

Statistics for the terms in the regression analysis for both lower and upper entrainment bounds (Fig. 5) are shown: *SS,* sum of squares; df_1, degrees of freedom for the term itself; *MS,* mean squares; *F, F* statistic; df_2, denominator degrees of freedom for the *F* test; *P,* probability. Significant effects are shown in bold.

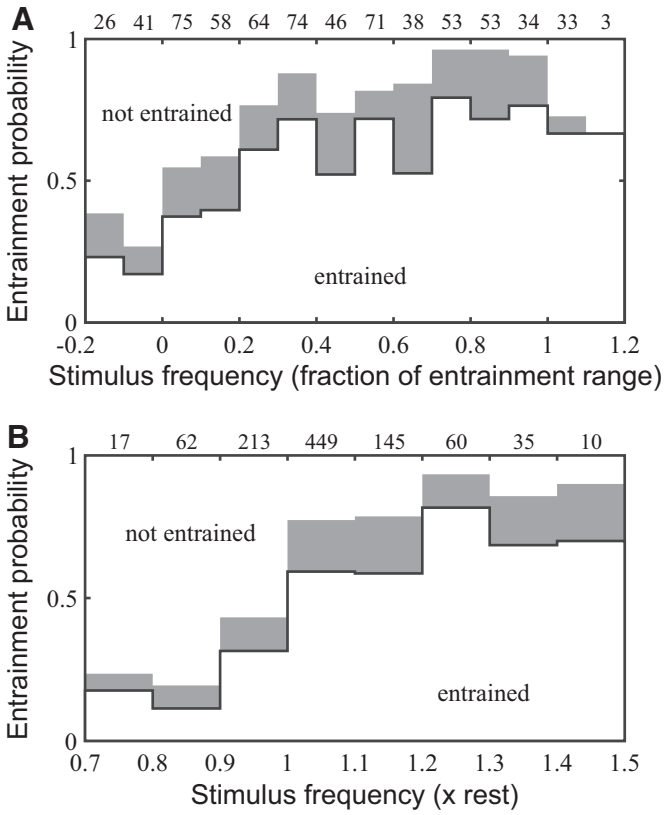

FIG. 6. The probability of entrainment varies over the entrainment range. In both plots, open bars show the probability of entrainment, estimated as the fraction of isolated trials that entrained for 30 stimulus cycles at a particular stimulus frequency. Gray bars show trials that were entrained at the end of 30 cycles, but not at the beginning, and thus might have entrained if the stimulus was applied for longer. Total number of trials in each bin is indicated along the *top* of the plot. *A*: fraction of trials at frequency binned over the entrainment range for a particular individual and stimulus position. *B*: fraction of trials at frequency binned relative to the resting burst frequency.

Fig. 7*C*, a histogram of data across all positions demonstrates that phase is bimodal.

These results are summarized in Fig. 7*D*, which shows the median and angular deviation of burst phase, grouped into five bins according to the position of the stimulus. Phases were significantly different among positions ($\chi^2_4 = 13.1$; $P = 0.011$). Pairwise comparisons indicated that the most rostral phase (bin 1) was significantly different from the two most caudal (bins 4 and 5), but that bins 2 and 3 were not significantly different from any of the others. The head and tail phases differed by 0.31, on average.

In contrast, whole and shortened preparations tended to produce the same phase values. Figure 7*B2* shows the phases from the shortened preparations (open symbols), compared with those from whole preparations (gray symbols). The median phases for the shortened preparations are summarized with open symbols in Fig. 7, *C* and *D*. Data from whole and shortened preparations were compared within each bin. No groups were significantly different (*P* values of 0.80, 0.41, and 0.15 for bins 2, 3, and 4, respectively).

Finally, the position of the stimulus relative to the electrode did not appear to affect the estimated burst phase. In Fig. 7*A*, squares (circles) indicate a stimulus above (below) the recording site. Too few data were available for a rigorous statistical test, but visual inspection suggests that the squares and circles follow the same general pattern.

The data shown in Fig. 7 are widely scattered. This scatter may in part reflect changes in the preparation over the course of the experiment. For example, suppose that the resting frequency was 0.8 Hz at the beginning of an experiment. However, after each trial of stimulation at 0.8 Hz, the resting frequency typically increased, so that whereas the first trial might have been at $1.0f_{rest}$, the fifth trial was at $0.95f_{rest}$. Some of the scatter in Fig. 7 may be due to this difficulty in bending the spinal cord precisely at its resting frequency. Thus the apparent variability of the phase values from central segments reflects the bimodality of phases, not differences in stimulation frequency.

To determine the robustness of the pattern shown in Fig. 7, we examined the effect of changes in stimulus frequency on the phase of entrainment. One reason the phases in Fig. 7 have some scatter is because the stimulus frequency was not precisely at the resting frequency. Because of the excitatory effect of bending, the resting frequency tended to increase over time, even within a single recording bout. It was therefore not feasible to bend the cord exactly at the resting frequency. To assess the effect of this methodological limitation, we estimated the slope of the phase change with respect to stimulus frequency (Fig. 8, *A* and *B1*) and multiplied that by the difference between the stimulus frequency and the rest frequency (Fig. 8*B2*) to estimate a deviation in phase (Fig. 8*B3*). The stimulus frequency used to produce Fig. 7*B* was $1.02 \pm 0.05f_{rest}$ (mean $\pm$ SD) and did not differ among stimulus positions [ANOVA; $F_{(4,59)} = 1.44$; $P = 0.23$; Fig. 8*B2*]. The resulting deviation was centered around zero (Fig. 8*B3*) and 95% of measurements had deviations within ± 0.13 of zero. The largest deviation was -0.27. All of the deviations were less than the phase difference between the head and the tail regions of the cord, which was 0.31. Therefore the pattern shown in Fig. 7 appears to be robust.

DISCUSSION

This study examines how bending stimuli can entrain the lamprey central pattern generator (CPG) and whether the entrainment response differs depending on the position of the stimulus along the spinal cord. We found two main differences along the spinal cord. First, bending near the center of a spinal cord preparation can entrain the CPG over almost twice the range of stimulus frequencies than bending at the ends (Fig. 5). Second, the phase relationship between CPG bursts and the bending stimulus is about 30% of a cycle different for bending at the head versus the tail end (Fig. 7). In the following text, we first discuss the entrainment range results, then we examine our phase results and their relationship to our two hypotheses.

Entrainment ranges

To the authors' knowledge, this is the first study to examine entrainment ranges as a function of stimulus position over a large portion of the spinal cord. Previous studies have examined entrainment ranges during bending at the rostral or caudal ends (McClellan and Sigvardt 1988; Williams et al. 1990). These studies both found that a rostral stimulus could entrain the spinal cord only above the resting frequency, whereas a

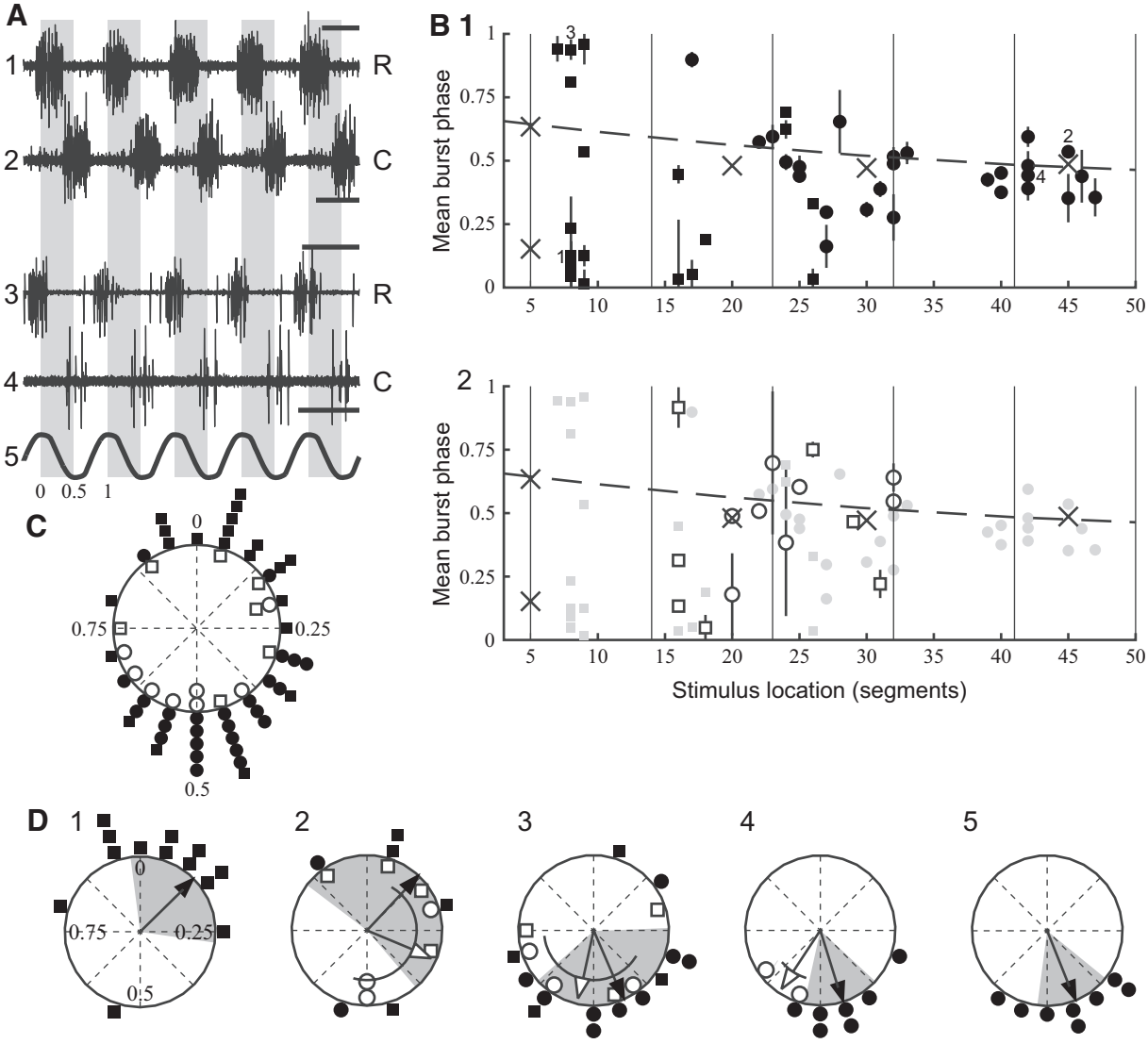

FIG. 7. Entrainment phase differs along the spinal cord. *A*: example bursts during bending at the resting frequency. *A1*, *A2*: rostral and caudal entrainment, respectively, for one individual. Rest frequency differs slightly between traces, but is about 0.57 Hz. *A3*, *A4*: rostral and caudal entrainment for another individual (rest frequency ~0.88 Hz). Scale bars are all equal to 1 s. *A5*: stimulus trace. Gray regions represent phase values from 0 to 0.5, equivalent to shortening on the side of the recording. *B*: mean entrainment phase at the resting frequency. The stimulus position relative to the electrode is shown with squares (circles) when the stimulus was below (above) the recording site. Error bars indicate angular SD. Previous in vitro measurements from Sigvardt and Williams (1989) and in vivo electromyographic (EMG) phase relationships from Williams et al. (1989) are shown with crosses and a dashed line, respectively. Vertical lines separate the bins for stimulus position used for the plots in *D*. *B1*: whole preparations (~50 segments) shown with filled symbols. Numbered points correspond to the traces shown in *A*. *B2*: shortened preparations shown with open symbols. Length of the preparations can be determined from the symbol. Squares (circles) indicate that the original 50-segment preparation was cut about 10 segments above (below) the stimulus location. Segment numbering is the same as in *panel 1*. To facilitate comparison, the data from *panel 1* are reproduced in gray in the background of *panel 2*. *C*: histogram of data from *B*. As before, closed (open) symbols represent whole (shortened) preparations, whereas squares (circles) indicate that the stimulus was below (above) the recording site. Phase is represented clockwise from *top*. Bin size is 0.05. Note the bimodal distribution. *D*: clock plots of phase data with angular medians and deviations for whole and shortened preparations, grouped into 5 regions according to stimulus position. Phase is shown as an angle measured clockwise from *top* (numbers shown on first clock). Filled (open) arrows represent the median phase for whole (shortened) preparations with a gray region (arc) to represent the deviation.

caudal stimulus could entrain both above and below the resting frequency. Our results do not show this asymmetry in entrainment ranges: we found no significant differences in the lower entrainment bound at any position along the spinal cord (Fig. 5 and Table 1). However, it is likely that the differences between our data and previous results reflect only methodological differences. In particular, our frequency sweep protocol is effective for rapidly determining approximate entrainment ranges, but is somewhat limited in its ability to detect subtle differences. Thus it showed the nearly twofold difference between entrainment at middle segments compared with that at rostral or caudal segments (Fig. 5), but did not detect smaller differences between rostral and caudal entrainment. Our experiments were designed mainly to examine phase at the resting burst frequency; more focused testing at the edges of the entrainment ranges would probably have shown differences in rostral and caudal segments.

However, despite the limitations of the frequency sweep protocol, our data clearly show that middle segments are different from the head and tail ends: bending at the center is

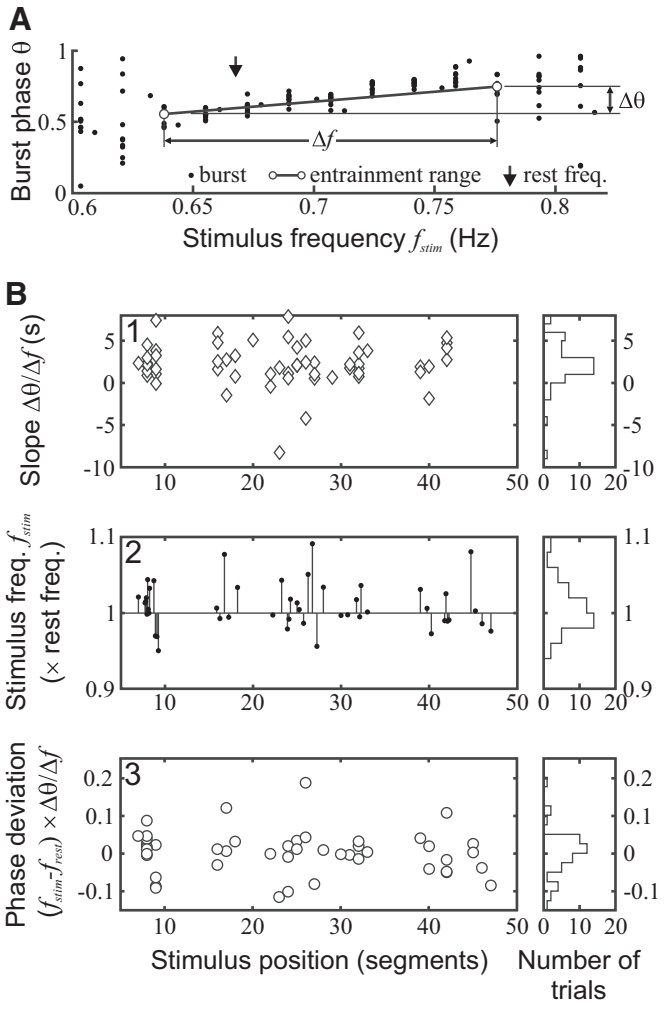

FIG. 8. Robustness check for rostral-to-caudal phase differences. For each frequency sweep, the change in phase $\Delta\theta$ over the entrainment range Δf was estimated. The resulting phase deviation was then estimated by by multiplying this slope $\Delta\theta/\Delta f$ by the difference in the stimulation frequency f_{stim} and the resting frequency f_{rest}. *A*: example frequency sweep showing the definitions of $\Delta\theta$ and Δf. *B*: an estimate of the deviation on phase estimates. For each panel, the *x*-axis is stimulus position in segments and a histogram is shown on the *right*. *1*: slope of the phase change with respect to frequency, estimated as $\Delta\theta/\Delta f$. *2*: stimulus frequency for phase values in Fig. 7*B1*, normalized by resting frequency. Lines are shown from each point to the resting frequency. *3*: deviation in the phase estimate in Fig. 7, estimated by multiplying the slope (*panel 1*) by the difference between the stimulus frequency and the resting frequency (*panel 2*).

able to entrain the CPG over a wider range of frequencies than bending at the ends. This result makes sense if one considers how segments are connected along the spinal cord. Segments are coupled one to another with both short- and long-distance connections, but the strength of the connections decreases over distance (Ayali et al. 2007; McClellan and Hagevik 1999; Miller and Sigvardt 2000). For a localized bending stimulus to entrain the entire spinal cord, the timing information must be distributed to the rest of the spinal cord through the intersegmental coordinating system. This could happen either fairly directly, through long-distance connections (thought to be 16 to 20 segments long in adult lampreys; Miller and Sigvardt 2000; Rovainen 1985; and ≤40 segments long in larval lampreys; McClellan and Hagevik 1999) or, indirectly, through short-distance connections across many segments. Either way, the signal will decrease in strength the further it has to go from the stimulus location. It thus seems clear that bending at middle segments should be able to entrain the cord more easily (Fig. 5), simply because the signal does not have to travel as far.

Finally, we found that entrainment is probabilistic over the estimated range of frequencies. When the entrainment range is defined using a frequency sweep, constant-frequency isolated trials at a frequency within that range usually cause entrainment, but sometimes do not. The entrainment range is therefore a region with high probability of entrainment, but the probability for 30-cycle trials is below unity (Fig. 6). Entrainment probability increases with increasing stimulus duration, but the pattern remains the same. In particular, entrainment is much less likely at the lower end of the entrainment range than at the higher end (Fig. 6*A*) and is less likely below the resting frequency than above it (Fig. 6*B*). This may reflect the slow excitatory effect of bending, as described by Kiemel and Cohen (2001; see also McClellan and Sigvardt 1988), and also observed in this study. Bending generally tends to increase the CPG frequency, even if the bending frequency is below the resting CPG frequency. For entrainment below the resting frequency, the entrainment effect and the excitatory effect will tend to oppose each other (Fig. 6*B*). At the high end of the entrainment range, however, the two effects reinforce each other, resulting in a much higher entrainment probability.

Phase

In freely swimming fishes, the phase between muscle activation and body bending differs at different points along the body (Wardle and Videler 1993; Wardle et al. 1995; Williams et al. 1989). These results suggested to us and to others that the phase of CPG bursting relative to a bending stimulus might also vary along the body.

Sigvardt and Williams (1989) described preliminary results investigating this hypothesis. Their results, given in summary in Williams et al. (1995) indicated that the CPG phase near the head was indeed different from that near the tail. The differences they observed followed approximately the same gradient seen in freely swimming fishes, except that they found two stable phase relationships at the rostral end of the spinal cord. Their published data are reproduced as crosses in Fig. 7.

Our data from tail segments show approximately the same pattern they reported, whereas data near the head are somewhat different (Fig. 7). We found that burst phase at the head end of the spinal cord was about 30% of a cycle later than burst phase at the tail end. Figure 9 illustrates the phase of CPG bursts, muscle activity, and body bending. Phase is defined following Sigvardt and Williams, so that 0 to 0.5 represents lengthening on the side where the electrode was recording and 0.5 to 1 represents shortening. The points in Fig. 7 represent the phase of burst centers; bursts typically span around 30% of a cycle (Wallén and Williams 1984). Thus the tail phase relationship represents a burst that begins during lengthening and continues into shortening, matching both the *in vivo* phase lag (dotted line in Fig. 7, after Williams et al. 1989) and the *in vitro* data of Sigvardt and Williams (crosses in Fig. 7).

Phase near the head represents activity beginning at the end of shortening and continuing well into the lengthening phase (Fig. 9). Sigvardt and Williams found two stable phase relationships at the rostral end. In contrast, the mean of our data

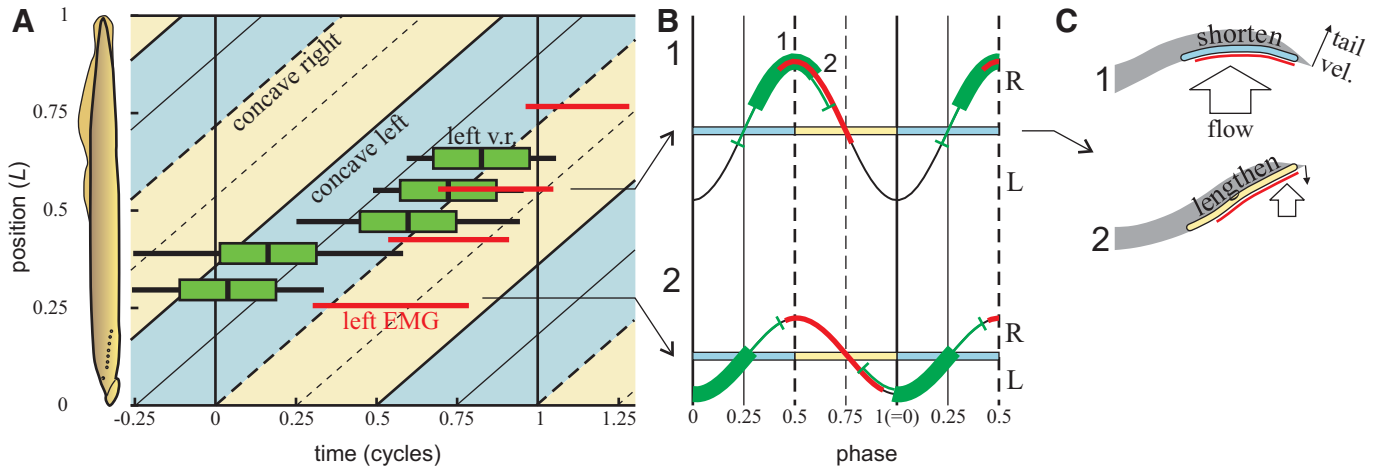

FIG. 9. Summary of current results and comparison with previous studies. *A*: diagram showing the timing of the left side ventral root bursts from the current study (green boxes) and left side electromyography data from swimming lampreys (red bars; data from Williams et al. 1989). In each box, the center black line and the error bars represent the mean timing and angular deviation of entrainment at the resting frequency (equivalent to data in Fig. 7*D*). Green boxes show the mean timing of central pattern generator bursts, assuming a burst duration of 30% of a cycle. The progression of the body wave is shown underneath in yellow and blue, using a body wavelength of 0.72*L* (Williams et al. 1989). Blue and yellow indicate left side lengthening and shortening, respectively. Phase values are shown with diagonal lines: thick solid lines are zero phase (fully concave to the left side), thick dashed lines are 50% phase (fully concave to the right side), and thin solid and dashed lines are 25 and 75% phase, respectively. *B*: schematic of body curvature (black curves), muscle activity (red lines), and ventral root bursts (green bars), plotted against phase. Two positions (*1*, caudal; *2*, rostral) from *A* are represented. Numbers indicate timing of schematics in *C*. Amplitude estimates from Wardle et al. (1995). *C*: schematic of tail motion and EMG activity shown in (*B1*). In *panel 1*, muscle has just become active (red bar) and the left side is shortening (blue bar), moving water ("flow") with the tail to the right ("tail vel."). In *panel 2*, the left side is beginning to lengthen and the tail is moving in the opposite direction, to the left. The water, however, continues to move to the right, producing a high pressure region on the tail. The muscle stays active to resist the pressure from the water.

matches just one of their points, the one that is furthest from the in vivo phase lag. We found no consistent rostral entrainment at a phase close to their second point or the in vivo phase lag. Our measurements, though, have a rather broad range (head deviation is almost twice the tail deviation; Fig. 7*B*). It may be that what Sigvardt and Williams observed was not two separate equilibrium phase values, but one broad and fairly flat equilibrium region.

Is the rostral-to-caudal phase gradient a real effect? Because phase is proportional to stimulus frequency (Fig. 8), a systematic bias toward higher frequencies for stimuli at the head could therefore produce a spurious correlation between stimulus position and burst phase. Several lines of evidence suggest this is not true and that the correlation is a real effect. First, there was no systematic bias in stimulus frequency at certain positions. Stimulus frequencies used to produce Fig. 7 did not differ among positions ($P = 0.25$; Fig. 8*B2*) and we randomized the order in which we tested different stimulus positions, so that there would not be a bias as the preparation changed over time. Even if there was a systematic bias, however, it would be unlikely to produce as large an effect as the one we observed. The error on the phase measurements that was attributable to misalignments between stimulus frequency and resting frequency was <0.13 in 95% of cases, but the phase difference from the head to the tail end of the spinal cord was typically around 0.3 cycle. Thus the differences shown in Fig. 7 are robust.

What could cause the observed difference in entrainment phase along the spinal cord? We proposed two hypotheses. The first hypothesis suggests that the gradient is a side effect of the preparation method. By cutting out the spinal cord in the dissection, we altered the balance of ascending and descending inputs at the rostral and caudal ends of the preparation, regardless of whether the excised segments came from the anatomically head or tail end of the animal. Under this hypothesis, we would expect phase to change if we cut the preparation and made it shorter. Alternatively, under the second hypothesis, anatomically rostral segments may respond differently than anatomically caudal segments to bending stimuli. Cutting the preparation would therefore not alter phase relationships.

Our data support the second hypothesis, not the first. Shortening the preparation did not alter the entrainment phase (compare Fig. 7*B1* to Fig. 6*B2* and closed to open arrows in Fig. 7*D*). Data from Sigvardt and Williams (1989) (reproduced as crosses in Fig. 7) also support the hypothesis that rostral and caudal segments differ in some way. They used both a rostral stimulus and a caudal stimulus on an approximately 50-segment preparation, then cut the preparation in half and applied rostral and caudal stimuli to each of the new ends (T. L. Williams, personal communication). Anatomically caudal segments entrained at a phase of about 0.5, like tail segments, not 0.2 like head segments, even when those segments were at the rostral end of the preparation.

Although our data strongly indicate that the rostral end of the lamprey spinal cord differs from the caudal end, they do not indicate what these anatomical differences may be. Many researchers have found variation in both the physiology and morphology of CPG interneurons (see, e.g., Buchanan 1982; Buchanan and Cohen 1982; Parker 2003; Rovainen 1974, 1982) as well as the edge cells themselves (Grillner et al. 1982; Viana Di Prisco et al. 1990). However, little is known whether these properties vary along the spinal cord and, if so, how they vary. Our results could be explained by differences in edge cell response properties along the spinal cord or by different edge cell connections. Due to their position on the lateral margin of the spinal cord, edge cells are difficult to record from. Thus after Viana Di Prisco et al. (1990) established the basic pattern, very few paired recordings have been conducted to determine

further details of edge cell connectivity. Also, inter- or intrasegmental connectivity differences may influence entrainment phase. For example, lateral interneurons are not present in the caudal regions of the spinal cord (Rovainen et al. 1973). Finally, rostral versus caudal differences in interneuron or motor neuron physiology (such as crossed caudal interneurons, which are known to vary substantially in their physiology; Buchanan 1982) could potentially produce the pattern we observed. Such gradients have not been investigated in the lamprey, but in *Xenopus* embryos, Tunstall and Roberts (1994) observed a gradient in synaptic drive to motoneurons and in several properties of motoneuron spiking.

Future studies at a cellular level will be needed to establish between the mechanism that results in the observed differences between rostral and caudal segments. Because our data show a fairly discrete transition (Fig. 7), it seems reasonable to speculate that there may be two separate rostral and caudal populations of cells, either edge cells or CPG interneurons, that have different response properties. Connectivity could also shift in a fairly discrete way along the spinal cord. These differences have implications for modeling of the lamprey CPG because segments are generally considered to be identical (e.g., in Cohen et al. 1982; Ekeberg and Grillner 1999; Williams 1992). Our results suggest that this assumption may not be valid.

Whatever the underlying mechanism, the estimated phase lag between stimuli and bursts near the head is different from that near the tail, but it also is about 20% of a cycle later than is observed during free swimming (Figs. 7 and 9). One possible explanation for the discrepancy is that the protocol used in this study was to bend the spinal cord at a single point, restricting the bending to one or two segments. During free swimming, however, the entire body bends. The effects of bending at multiple points may not be equivalent to adding up the effects of bending at each point individually. In particular, since the body wave is continuous, it cannot have abrupt changes in phase. The body mechanics during normal swimming may therefore serve to smooth out the phase gradient shown in Fig. 9 and force it toward the values observed in vivo.

If body mechanics serve to smooth out the phase relationships observed in this study, do our observations then have any functional consequences? In fact, the broad equilibrium phase at the head end of the spinal cord may represent a functional difference between the head and tail. At the tail end, the burst phases are narrowly distributed at the appropriate phase for effective transmission of forces to the fluid (Fig. 9, *B* and *C*). The dominant fluid force at the tail will be the acceleration reaction: the fluid, like anything with mass, resists acceleration and deceleration. When the tail begins to slow down as it reaches its maximum excursion (Fig. 9*C1*), the fluid will resist the deceleration. Tail muscles must therefore turn on as they are lengthening, to stiffen the tail and counteract the acceleration reaction (Fig. 9*C2*) (Blight 1977); otherwise, the tail would flop over to one side. Thus the phase of tail muscle activity helps to determine the angle of the tail in the flow, which is quite important for effective force production (Lighthill 1971). Not only that, force is probably rather sensitive to small changes in phase, if they affect the tail angle. Engineering studies have shown that flapping propulsors like fish tails can produce rather different fluid flows, depending on the phase relationship between their angle and the side-to-side motion (Akhtar and Mittal 2005; Gopalkrishnan et al. 1994; Hover et al. 2004). At the head end, by contrast, relatively little force is produced during steady swimming (Kern and Koumoutsakos 2006), so the phase of muscle activity may not be so important for force production. However, both turns and accelerations are initiated by changes in rostral kinematics (Fagerstedt and Ullén 2001; Tytell 2004). Thus the animal will need more flexibility in the motor program closer to its head. The broad rostral phase distribution may be a sign of this flexibility.

ACKNOWLEDGMENTS

We thank A. Ayali, T. Williams, P. Holmes, T. Kiemel, K. Hoffman, and J. Buchanan. S. Gelman, L. Tucker, and K. Nepote helped maintain the animals. R. Wood provided much useful advice on the machining of the bath and bending apparatus. Three anonymous reviewers helped to substantially improve the manuscript.

GRANTS

This work was supported by a Ruth L. Kirschstein National Research Service Award/National Institute of Neurological Disorders and Stroke (NINDS) Grant F32 NS-054367 to E. D. Tytell and Collaborative Research in Computational Neuroscience/NINDS Grant R01 NS-05427102 to A. H. Cohen.

REFERENCES

Akhtar I, Mittal R. A biologically inspired computational study of flow past tandem flapping foils. *AIAA J* 2005-4760: 1–12, 2005.

Ayali A, Fuchs E, Ben-Jacob E, Cohen A. The function of intersegmental connections in determining temporal characteristics of the spinal cord rhythmic output. *Neuroscience* 147: 236–246, 2007.

Blight AR. The muscular control of vertebrate swimming movements. *Biol Rev* 52: 181–218, 1977.

Bone Q. Locomotor muscle. In: *Fish Physiology*, edited by Hoar WS, Randall DJ. New York: Academic Press, 1978, p. 361–424.

Buchanan JT. Identification of interneurons with contralateral, caudal axons in the lamprey spinal cord: synaptic interactions and morphology. *J Neurophysiol* 47: 961–975, 1982.

Buchanan JT, Cohen AH. Activities of identified interneurons, moto-neurons, and muscle-fibers during fictive swimming in the lamprey and effects of reticulospinal and dorsal cell stimulation. *J Neurophysiol* 47: 948–960, 1982.

Cohen AH. Effects of oscillator frequency on phase-locking in the lamprey central pattern generator. *J Neurosci Methods* 21: 113–125, 1987.

Cohen AH, Holmes PJ, Rand RH. The nature of the coupling between segmental oscillators of the lamprey spinal generator for locomotion—a mathematical model. *J Math Biol* 13: 345–369, 1982.

Cohen AH, Wallén P. The neuronal correlate of locomotion in fish. "Fictive swimming" induced in an in vitro preparation of the lamprey spinal cord. *Exp Brain Res* 41: 11–18, 1980.

Ekeberg Ö, Grillner S. Simulations of neuromuscular control in lamprey swimming. *Philos Trans R Soc Lond B Biol Sci* 354: 895–902, 1999.

Fagerstedt P, Ullén F. Lateral turns in the lamprey. I. Patterns of motoneuron activity. *J Neurophysiol* 86: 2246–2256, 2001.

Fisher NI. *Statistical Analysis of Circular Data.* Cambridge, UK: Cambridge Univ. Press, 1995.

Gopalkrishnan R, Triantafyllou MS, Triantafyllou GS, Barrett D. Active vorticity control in a shear flow using a flapping foil. *J Fluid Mech* 274: 1–21, 1994.

Gossard JP. Control of transmission in muscle group IA afferents during fictive locomotion in the cat. *J Neurophysiol* 76: 4104–4112, 1996.

Grillner S. On the generation of locomotion in the spinal dogfish. *Exp Brain Res* 20: 459–470, 1974.

Grillner S. Central pattern generators for locomotion, with special reference to vertebrates. *Ann Rev Neurosci* 8: 233–261, 1985.

Grillner S, McClellan A, Sigvardt K. Mechanosensitive neurons in the spinal-cord of the lamprey. *Brain Res* 235: 169–173, 1982.

Grillner S, Williams T, Lagerback P-A. The edge cell, a possible intraspinal mechanoreceptor. *Science* 223: 500–503, 1984.

Guan L, Kiemel T, Cohen AH. Impact of movement and movement-related feedback on the lamprey central pattern generator for locomotion. *J Exp Biol* 204: 2361–2370, 2001.

Hagevik A, McClellan AD. Coordination of locomotor activity in the lamprey: role of descending drive to oscillators along the spinal cord. *Exp Brain Res* 128: 481–490, 1999.

Hatsopoulos NG, Warren WHJ. Resonance tuning in rhythmic arm movements. *J Motor Behav* 28: 3–14, 1996.

Hover FS, Haugsdal O, Triantafyllou MS. Effect of angle of attack profiles in flapping foil propulsion. *J Fluids Struct* 19: 37–47, 2004.

Iwasaki T, Zheng M. Sensory feedback mechanism underlying entrainment of central pattern generator to mechanical resonance. *Biol Cybern* 94: 245–261, 2006.

Kern S, Koumoutsakos P. Simulations of optimized anguilliform swimming. *J Exp Biol* 209: 4841–4857, 2006.

Kiemel T, Cohen AH. Estimation of coupling strength in regenerated lamprey spinal cords based on a stochastic phase model. *J Comput Neurosci* 5: 267–284, 1998.

Kiemel T, Cohen AH. Bending the lamprey spinal cord causes a slowly-decaying increase in the frequency of fictive swimming. *Brain Res* 900: 57–64, 2001.

Kiemel T, Gormley KM, Guan L, Williams TL, Cohen AH. Estimating the strength and direction of functional coupling in the lamprey spinal cord. *J Comput Neurosci* 15: 233–245, 2003.

Lighthill J. Large-amplitude elongated-body theory of fish locomotion. *Proc R Soc Lond B Biol Sci* 179: 125–138, 1971.

Marder E, Bucher D. Central pattern generators and the control of rhythmic movements. *Curr Biol* 11: R986–R996, 2001.

McClellan AD, Hagevik A. Coordination of spinal locomotor activity in the lamprey: long-distance coupling of spinal oscillators. *Exp Brain Res* 126: 93–108, 1999.

McClellan AD, Jang WC. Mechanosensory inputs to the central pattern generators for locomotion in the lamprey spinal cord: resetting, entrainment, and computer modeling. *J Neurophysiol* 70: 2442–2454, 1993.

McClellan AD, Sigvardt K. Features of entrainment of spinal pattern generators for locomotor activity in the lamprey. *J Neurosci* 8: 133–145, 1988.

McMahon TA. *Muscles, Reflexes, and Locomotion.* Princeton, NJ: Princeton Univ. Press, 1984.

Miller WL, Sigvardt KA. Extent and role of multisegmental coupling in the lamprey spinal locomotor pattern generator. *J Neurophysiol* 83: 465–476, 2000.

Milliken GA, Johnson DE. *Analysis of Messy Data. 3. Analysis of Covariance.* Boca Raton, FL: CRC Press, 2001.

Parker D. Variable properties in a single class of excitatory spinal synapse. *J Neurosci* 23: 3154–3163, 2003.

Pearson KG. Proprioceptive regulation of locomotion. *Curr Opin Neurobiol* 5: 786–791, 1995.

Rome LC, Swank D, Corda D. How fish power swimming. *Science* 261: 340–343, 1993.

Rovainen CM. Synaptic interactions of identified nerve cells in the spinal cord of the sea lamprey. *J Comp Neurol* 154: 189–206, 1974.

Rovainen CM. Neurophysiology. In: *The Biology of Lampreys*, edited by Hardisty MW, Potter IC. London: Academic Press, 1982, p. 1–136.

Rovainen CM. Effects of groups of propriospinal interneurons on fictive swimming in the isolated spinal cord of the lamprey. *J Neurophysiol* 54: 959–977, 1985.

Rovainen CM, Johnson PA, Roach EA, Mankovsky JA. Projections of individual axons in lamprey spinal cord determined by tracings through serial sections. *J Comp Neurol* 149: 193–201, 1973.

Sigvardt K, Williams TL. Phase coupling during entrainment of fictive locomotion in the lamprey spinal cord. *Soc Neurosci Abstr* 14: 258, 1989.

Tunstall MJ, Roberts A. A longitudinal gradient of synaptic drive in the spinal cord of Xenopus embryos and its role in co-ordination of swimming. *J Physiol* 474: 393–405, 1994.

Tytell ED. Kinematics and hydrodynamics of linear acceleration in eels, Anguilla rostrata. *Proc R Soc Lond B Biol Sci* 271: 2535–2541, 2004.

Tytell ED, Cohen AH. Phase lags between muscle activity and movement in the lamprey: contribution of the central pattern generator. Program No. 78.14. *2007 Abstract and Itinerary Planner*. Washington, DC: Society for Neuroscience, 2007. Online.

Viana Di Prisco G, Wallén P, Grillner S. Synaptic effects of intraspinal stretch-receptor neurons mediating movement-related feedback during locomotion. *Brain Res* 530: 161–166, 1990.

Vinay L, Barthe JY, Grillner S. Central modulation of stretch receptor neurons during fictive locomotion in lamprey. *J Neurophysiol* 76: 1224–1235, 1996.

Wallén P, Williams TL. Fictive locomotion in the lamprey spinal cord in vitro compared with swimming in the intact and spinal animal. *J Physiol* 347: 225–239, 1984.

Wardle CS, Videler JJ. The timing of the electromyogram in the lateral myotomes of mackerel and saithe at different swimming speeds. *J Fish Biol* 42: 347–359, 1993.

Wardle CS, Videler JJ, Altringham JD. Tuning in to fish swimming waves: body form, swimming mode and muscle function. *J Exp Biol* 198: 1629–1636, 1995.

Williams CA, DeWeerth SP. A comparison of resonance tuning with positive versus negative sensory feedback. *Biol Cybern* 96: 603–614, 2007.

Williams T, Grillner S, Smoljaninov VV, Wallén P, Kashin S, Rossignol S. Locomotion in lamprey and trout: the relative timing of activation and movement. *J Exp Biol* 143: 559–566, 1989.

Williams TL. Phase coupling by synaptic spread in chains of coupled neuronal oscillators. *Science* 258: 662–665, 1992.

Williams TL, Bowtell G, Carling J, Sigvardt K, Curtin NA. Interactions between muscle activation, body curvature and the water in the swimming lamprey. In: *Biological Fluid Dynamics*, edited by Ellington CP, Pedley TJ. Cambridge, UK: Company of Biologists, 1995, p. 49–59.

Williams TL, Sigvardt KA, Kopell N, Ermentrout GB, Remler MP. Forcing of coupled nonlinear oscillators: studies of intersegmental coordination in the lamprey locomotor central pattern generator. *J Neurophysiol* 64: 862–871, 1990.

Zar JH. *Biostatistical Analysis.* Upper Saddle River, NJ: Prentice Hall, 1999.